Analysis of Strehl ratio limit with superresolution binary phase filters

Vidal F. Canales*, Pedro J. Valle, and Manuel P. Cagigal

Departamento de Física Aplicada, Universidad de Cantabria, Santander 39005, Spain
**Corresponding author: fernancv@unican.es*

Received February 26, 2016; accepted May 5, 2016; posted online June 13, 2016

Several pupil filtering techniques have been developed in the last few years to obtain transverse superresolution (a narrower point spread function core). Such a core decrease entails two relevant limitations: a decrease of the peak intensity and an increase of the sidelobe intensity. Here, we calculate the Strehl ratio as a function of the core size for the most used binary phase filters. Furthermore, we show that this relation approaches the fundamental limit of the attainable Strehl ratio at the focal plane for any filter. Finally, we show the calculation of the peak-to-sidelobe ratio in order to check the system viability in every application.

OCIS codes: 100.6640, 110.1220, 350.5730.
doi: 10.3788/COL201614.071101.

The term superresolution has been widely used in scientific literature with two different meanings: the increase of the spatial frequency cutoff in an optical system, on one hand, and the increase of the generalized Rayleigh resolution on the other. Here, we will use the latter meaning, introduced in the classical works by Toraldo di Francia[1], which can also be associated with a decrease of the point spread function (PSF) core width. Such a decrease can be useful in many applications[2–6], and has been analyzed in many works[7–9]. The first attempts of PSF engineering were related to amplitude filters, but in recent years phase and hybrid designs[9,10] (including ternary optical elements[11,12]) have been developed due to their better performance in most applications[13,14]. Among all filters, binary 0-π phase filters[15] stand out because they do not produce focus displacement, achieve excellent performances, allow several analytical results, and are easily fabricated. For these reasons they have been proposed for several applications[16–19]. Moreover, as will be seen, these filters provide the highest PSF peak for a certain resolution without focus displacement.

Toraldo di Francia already realized that theoretically an optical instrument with a given pupil size can yield as a narrow a PSF core as desired, but with the unavoidable cost of energy loss. The quantification of such energy loss is of utmost relevance because it can determine the viability of a technique in an application. In the crucial case of binary 0-π filters, this limit has been estimated analytically[15] by using parabolic approximation. Such approximation is not accurate enough, so the main goal of this work is to obtain a more accurate calculation of energy loss for such filters, which are the ones used most because of their known excellent performance.

Moreover, we will demonstrate that, for a given peak height, binary two-zone 0-π phase filters yield the best resolution at the focal plane of all real filters. Hence, this relation between the energy loss and the resolution can be considered as a fundamental limit for such a filter's performance (at this point we must note that we are considering systems with rotational symmetry). This limit is relevant for practical and theoretical reasons. The best attempts to derive a fundamental limit was performed by Sales and Morris[20,21], who derived an upper bound for the Strehl ratio limit from an expansion of the Bessel function of order zero in the expression of the field at the focal plane. This theoretical bound works very well for low Strehl values, though it overestimates the limit for higher values, so Sales and Morris solved this issue by substituting a region of their curve by a linear fit based precisely on 0-π binary filters. Here, we will derive the limit in a different way, which has results that are even a bit more restrictive. To this aim, we will follow this scheme. First, we will derive the relation between resolution and energy loss by using common figures of merit. Secondly, we will demonstrate that 0-π filters yield the highest peak for a fixed resolution of all two-zone filters. Then, we will demonstrate that two-zone filters outperform filters with a higher number of zones (which includes continuous filters). These demonstrations show that 0-π filters outperform any other real filter, which means that the calculated relation is a fundamental limit for the pupil filtering techniques with no focus displacement. Furthermore, the comparison of 0-π filters with complex filters is discussed. Finally, resolution improvement gives rise not only to a Strehl decrease, but also to an increase in the sidelobe intensity[22]. In most applications, the sidelobe height is as crucial as the Strehl ratio and the resolution to make a technique viable. Consequently, we show the calculation of the peak-to-sidelobe ratio corresponding to the limit case.

In order to relate the resolution and the energy loss, we need some figures of merit that describe the PSF. We have chosen the same figures of merit as Sales and Morris: the Strehl ratio S, defined as the ratio of the intensity at the focal point corresponding to an unobstructed pupil, and the normalized spot size G, which is the ratio of the radius of the first zero of the superresolving diffraction pattern to

that of the Airy pattern. In addition, we will also analyze the peak-to-sidelobe ratio Γ in order to check the performance of the filters [in most applications low values of Γ (<10) are not acceptable]. In addition, it must be noted that in real applications, the sidelobe may be reduced through hybrid filters[9] or nonlinear effects[23].

The first step is the derivation of the Strehl ratio limit for 0-π filters. Let us consider a general complex pupil function $P(\rho)$ (with rotational symmetry), where ρ is the normalized radial coordinate. For a converging monochromatic spherical wave front passing through the center of the pupil, the normalized field amplitude U in the focal plane may be written as[24]

$$U(v) = 2\int_0^1 P(\rho) J_0(v\rho)\rho \mathrm{d}\rho, \tag{1}$$

where J_n represents a Bessel function of the first kind (0th order in this case), v is the radial dimensionless optical coordinate at the focal plane given by $v = k$ NA r with $k = 2\pi/\lambda$, NA is the numerical aperture of the pupil, and r is the usual radial distance. In the case of 0-π binary phase filters with two zones [$P(\rho) = -1$ if $\rho < \rho_1$ and one if $\rho_1 < \rho < 1$], the integral in Eq. (1) yields:

$$U(v) = 2\left(\frac{J_1(v)}{v} - 2\rho_1 \frac{J_1(\rho_1 v)}{v}\right), \tag{2}$$

where ρ_1 is the normalized radius of the first zone (note that a similar expression for n-zone phase filters can be found in Ref. [22]). The core width is given by the position of the first zero, $v_0 = v_{0\mathrm{Airy}}$ $G = 1.22\pi$ $G = 3.83$ G. At this position the following equation must be fulfilled:

$$J_1(3.83G) = 2\rho_1 J_1(3.83G\rho_1). \tag{3}$$

The core height is given by the Strehl ratio:

$$S = |U(0)|^2 = (1 - 2\rho_1^2)^2. \tag{4}$$

From Eqs. (3) and (4), the resolution and intensity of the PSF core can be related. Equation (3) can be solved numerically for each G, while the corresponding S can be obtained from Eq. (4) [it must be noted that the curves of $S(\rho_1)$ and $G(\rho_1)$ can be found in Ref. [25], but not $S(G)$, the main goal of this work, which is a very relevant relationship for the analysis of filter performance].

Furthermore, it is very interesting to expand the Bessel function, J_1, in the second term of Eq. (3), in order to derive analytical expressions. It allows us to avoid the numerical resolution of Eq. (3) and, consequently, to obtain a direct expression of $S(G)$, which yields an easier and deeper understanding of system behavior. If the first two terms of the expansion are used, then Eq. (3) can be solved by

$$\rho_1 = \frac{2}{3.83G}\left[1 - \left(1 - \frac{3.83GJ_1(3.83G)}{2}\right)^{1/2}\right]^{1/2}, \tag{5}$$

and the analytical expression between S and G can be found from Eq. (4):

$$S = \left\{1 - 2\left(\frac{2}{3.83G}\right)^2\left[1 - \left(1 - \frac{3.83GJ_1(3.83G)}{2}\right)^{1/2}\right]\right\}^2. \tag{6}$$

Higher order terms can be used. With three terms of the J_1 expansion, the radius can be derived and the corresponding Strehl ratio is

$$S = \left\{1 - 2\left(\frac{2}{3.83G}\right)^2 \times \left[2 - \left(1 - \sqrt{3}i\right)\left(-1 + \frac{3}{8}3.83GJ_1(3.83G)\right)^{1/3}\right]\right\}^2. \tag{7}$$

Note that Eq. (7), in spite of the complex numbers, is always real. Figure 1 shows these expressions of S as a function of the core size G. It can be seen that the fit with the exact curve of the approximation with two terms is very good. The use of the three-term approximation entails a slight improvement. As a consequence, both can be useful for system analysis. Furthermore, if these curves are compared with the parabolic approximation for 0-π filters[15], it can be seen that such approximation is too restrictive, and that the new derived relationship between energy loss and resolution, as shown in Eq. (7), is more accurate.

On the other hand, when comparing these curves with the upper bound for general filters[20], one could wonder if 0-π filters were far from optimum behavior. However, we are going to demonstrate that 0-π filters outperform other filters, and consequently, the derived curve seems to be a

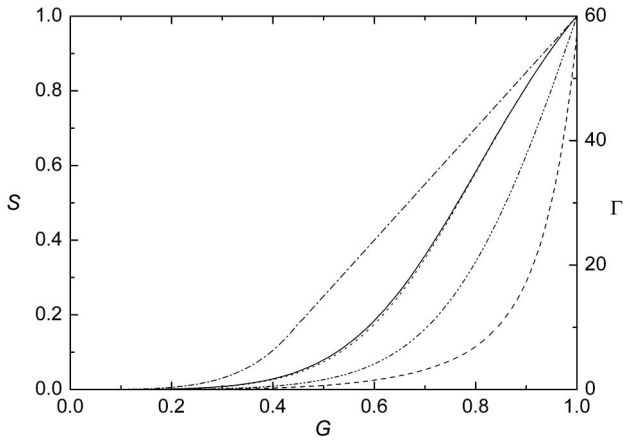

Fig. 1. Strehl ratio (solid curve) as a function of the core size. The approximations given by Eq. (6) (dotted curve) and Eq. (7) (short dashed-dotted curve) are also shown. Note that the latter is indistinguishable from the exact one. The Strehl ratio limit by Sales and Morris (dash-dotted curve) and by the parabolic approximation (dash-dot-dotted curve) are also shown for comparison. Finally, the peak-to-sidelobe ratio (dashed curve) for 0-π filters is shown in the secondary axis.

fundamental limit for filter performance. Let us begin the comparison with other filters. First, we choose two-zone real filters, which can be represented by

$$P(\rho) = \begin{cases} t & 0 \le \rho \le \rho_1 \\ 1 & \rho_1 < \rho \le 1 \end{cases}, \tag{8}$$

where t is the transmittance of the inner zone. Amplitude filters correspond to $t \ge 0$ while phase and hybrid filters present $t < 0$. Note that we have chosen t in the inner zone (such choice seems almost evident, and it can be demonstrated that it is the best option in a very similar way to the rest of demonstration of this work). The field at the focal plane becomes

$$U(v) = 2\left(\frac{J_1(v)}{v} - (1-t)\rho_1 \frac{J_1(\rho_1 v)}{v}\right). \tag{9}$$

The corresponding Strehl ratio is $S = [1-(1-t)\rho_1^2]^2$. From this expression it can be seen that for a fixed S if t increases the radius increases. So, the minimum radius is reached for $t = -1$, the pure phase filter. Taking into account the behavior of $J_1(\rho_1 v)$ (whose width decreases with increasing ρ_1) the second term in Eq. (9) is widest for $t = -1$, and hence, the resolution is maximum for $t = -1$, as shown in Fig. 2 (it can be seen that the wider the second term, the sooner it equals the first term, giving a zero of the total field). Conversely, for a fixed resolution, the maximum S of all real two-zone filters is obtained by pure phase filters.

Now, we shall demonstrate that the addition of zones does not improve the Strehl ratio attained with the two-zone filters for a given resolution, as already suggested in previous works[9,20] (such multizone filters can still be interesting because they yield a higher number of solutions and, thus, more flexibility[26]). Let us consider a three-zone filter with radii ρ_1 and ρ_2 (for simplicity we consider that the intermediate zone has $t = -1$, without the loss of generality). From Eq. (1) (or from Ref. [17]) its field is

$$U(v) = \frac{2J_1(v)}{v} - 4\left(\rho_2 \frac{J_1(\rho_2 v)}{v} - \rho_1 \frac{J_1(\rho_1 v)}{v}\right). \tag{10}$$

Then we consider a two-zone filter with the same Strehl ratio as the three-zone filter (it is easy to derive from Eqs. (4) and (10) that the corresponding radius is $\rho_{1b} = (\rho_2^2 - \rho_1^2)^{1/2}$). Now, the term inside the brackets in Eq. (10) is obviously narrower and lower than $J_1(\rho_2 v)$, but the corresponding term of the two-zone filter, $J_1(\rho_{1b} v)$, is wider than $J_1(\rho_2 v)$ (again due to the uniform behavior of $J_1(\rho v)$ with ρ). This means, as can be seen in Fig. 3, that $J_1(\rho_{1b} v)$ cuts the first term $(J_1(v)/v)$ before the term in brackets does [such cuts are the zeros of $U(v)$] Consequently, the two-zone filter will present a better resolution than the three-zone filter. Conversely, if we fix the resolution, the two-zone filter will present the highest Strehl ratio. The same reasoning used for three-zone filters can be applied for a higher number of zones and continuous filters.

The two latter demonstrations can be combined to show that two-zone 0-π filters reach the best possible performance of all filters without focus displacement, which converts the derived expression of $S(G)$ into a fundamental limit for superresolution performance.

The previous conclusion is very important because real filters are the most common filters. Nonetheless, the comparison of 0-π filters with general (complex) filters is of great interest. The analytical study of the PSF of complex filters is extremely difficult because there is focus displacement, and consequently, instead of Bessel functions as in real filters, Lommel functions (which are an infinite series of Bessel functions) must be used[24]. We have, thus,

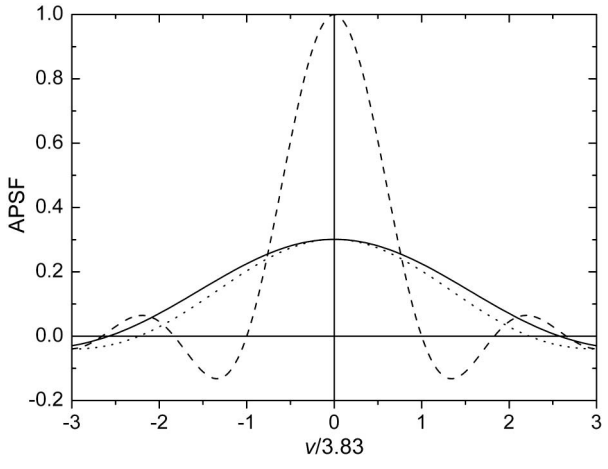

Fig. 2. Amplitude PSF for a clear pupil of radius 1, i.e., the first term of Eq. (9) (dashed curve), which acts as a reference. The second term of Eq. (9) is shown for $t = -1$ (solid curve) and $t = 0.5$ (dotted curve). For any t value, the first zero of the PSF is the point where its corresponding second term equals the reference.

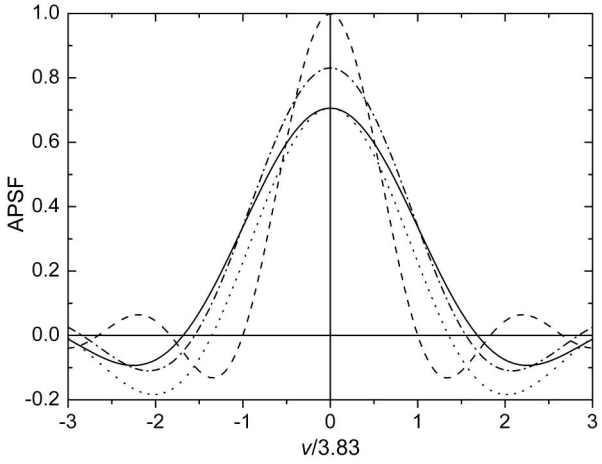

Fig. 3. Amplitude PSF for a clear pupil of radius 1, i.e., the first term of Eq. (10) (dashed curve). The second term of Eq. (10) is shown for two-zone filters of radius ρ_2 (dash-dotted curve) and ρ_{1b} (solid curve), and for a three-zone filter of radii ρ_1 and ρ_2 (dotted curve).

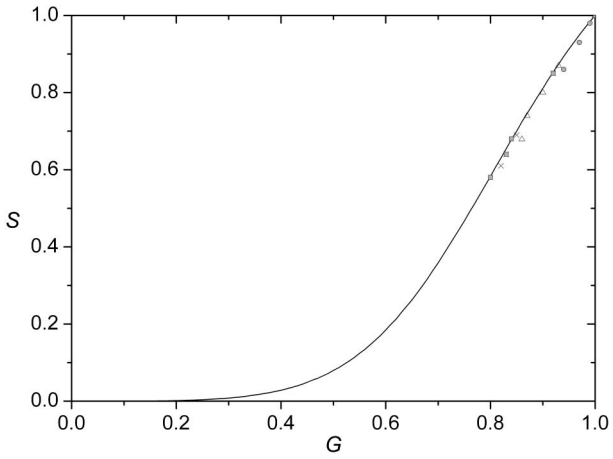

Fig. 4. Strehl ratio as a function of the core size for two-zone phase filters with a different phase difference: $\pi/2$ (circles), $3\pi/4$ filters (triangles), $7\pi/8$ filters (crosses), $15\pi/16$ (squares) and π (solid curve).

studied the case numerically. For such a study, we have chosen two-zone phase filters with a phase difference other than π (this is a relevant case, because the conclusions can be generalized for filters with attenuation or a higher number of zones as in previous sections). In Fig. 4, the Strehl ratio attainable as a function of resolution for different phase values is shown. It can be seen that no two-zone filter outperforms the 0-π filter for any resolution. Besides, it can be seen that the only filters able to yield any desired resolution are 0-π filters: the rest of them reach a resolution limit, which is higher as the phase difference between phase zones approaches π. The case of general continuous phase filters with focus displacement is out of the scope of this work (though generalization of these results suggests that binary 0-π filters will not be outperformed at the focal plane).

Finally, in order to complete the filter analysis, we show the behavior of the peak-to-sidelobe ratio Γ, which is an important parameter in filter design[8,20]. The position of the first lobe maximum, v_M, of the PSF can be obtained by deriving the field in Eq. (1), which leads to

$$J_2(v_M) = 2\rho_1^2 J_2(v_M\rho_1). \tag{11}$$

Once this position is known, $\Gamma = \mathrm{PSF}(0)/\mathrm{PSF}(v_M)$ can be calculated. Its behavior is shown in Fig. 1. Note that this figure shows both S and Γ as a function of the resolution, and thus, it is a representation of the performance limits of pupil filters and is a key to decide the viability of superresolution techniques in any application.

In conclusion, we calculate more precisely than in our precious works the Strehl ratio as a function of the core size in the crucial case of binary 0-π filters. Then, we show that, for the same resolution, real filters (the most relevant kind of filter) cannot yield a higher Strehl ratio at the focal plane than 0-π two-zone filters. Furthermore, by numerical analysis, no two-zone complex filter outperforms 0-π two-zone filters. Finally, we include in the analysis the sidelobe height, so that the most relevant limits for filter performance can be easily appreciated, which is useful for filter design.

This work was supported by the by the Ministerio de Economía y Competitividad under project FIS2012-31079.

References

1. G. Toraldo di Francia, Nuovo Cimento Suppl. **9**, 426 (1952).
2. M. Martínez-Corral, P. Andrés, C. J. Zapata-Rodríguez, and M. Kowalczyk, Opt. Commun. **165**, 267 (1999).
3. V. F. Canales, D. M. de Juana, and M. P. Cagigal, Opt. Lett. **29**, 935 (2004).
4. X. Zhao, C. Li, and H. Ruan, Opt. Eng. **44**, 125202 (2005).
5. S. Pereira and A. S. van de Nes, Opt. Commun. **234**, 119 (2004).
6. J. Jia, C. Zhou, and L. Liu, Opt. Commun. **228**, 271 (2003).
7. D. M. de Juana, J. E. Oti, V. F. Canales, and M. P. Cagigal, Opt. Lett. **28**, 607 (2003).
8. C. J. R. Sheppard, S. Ledesma, J. Campos, and J. Escalera, Opt. Lett. **32**, 1713 (2007).
9. P. Narayan, E. Hack, and P. Rastogi, Opt. Express **13**, 2835 (2005).
10. V. F. Canales and M. P. Cagigal, Opt. Express **14**, 10393 (2006).
11. Y. Zha, J. Wei, H. Wang, and F. Gan, J. Opt. **15**, 075703 (2013).
12. J. Wei, Y. Zha, and F. Gan, Prog. Electromag. Res. **140**, 589 (2013).
13. H. Luo and C. Zhou, Appl. Opt. **43**, 6242 (2004).
14. H. Ding, Q. Li, and W. Zou, Opt. Commun. **229**, 117 (2004).
15. V. F. Canales, J. E. Oti, and M. P. Cagigal, Opt. Commun. **247**, 11 (2005).
16. J. Yu, C. Zhou, and W. Jia, Opt. Commun. **283**, 4171 (2010).
17. V. F. Canales, P. J. Valle, J. E. Oti, and M. P. Cagigal, Chin. Opt. Lett. **7**, 720 (2009).
18. S. Wang, X. Zhao, and C. Zhao, Opt. Commun. **290**, 8 (2013).
19. Y. Zha, J. Wei, and F. Gan, Opt. Commun. **293**, 139 (2013).
20. T. R. M. Sales and G. M. Morris, Opt. Lett. **22**, 582 (1997).
21. T. R. M. Sales, Phys. Rev. Lett. **81**, 3844 (1998).
22. S. Mukhopadhyay and L. Hazra, Appl. Opt. **54**, 9205 (2015).
23. Y. Zha, J. Wei, and F. Gan, Opt. Commun. **304**, 49 (2013).
24. M. Born and E. Wolf, *Principles of Optics*, 7th ed. (Cambridge University Press, 2003).
25. T. R. M. Sales and G. M. Morris, J. Opt. Soc. Am. A **14**, 1637 (1997).
26. D. Mugnai, A. Ranfagni, and R. Ruggeri, Phys. Lett. A **311**, 77 (2003).